Research Article

Low-temperature synthesis of micro- and nano-crystalline $CuFeS_2$ polymorphs

Balamurugan Karuppannan[1,2,3] · Jacqueline L. Sturgeon[4] · Kristin L. Bunker[4] · Karen E. Harris[4] · Ravi Ganesan[3] · Jennifer A. Aitken[1]

Received: 3 July 2020 / Accepted: 16 October 2020 / Published online: 31 October 2020

Abstract
Micro- and nano-crystalline polymorphs of $CuFeS_2$ have been synthesized by using simple, low temperature solvothermal and precipitation methods. A solvothermal process at 170 °C, using ethylenediamine produced micro- and nano-crystalline $CuFeS_2$ with various shapes and morphologies, which include polygons, pyramids, hexagonal rods and plates etc. In addition to the expected tetragonal, chalcopyrite phase, a new, relatively low symmetry, hexagonal, wurtzite phase of $CuFeS_2$ was also obtained. The wurtzite phase fraction was found to be ~21 wt% by Rietveld analysis using X-ray powder diffraction data. Further, the effects of solvent concentration, reaction temperature and annealing on the crystallites have been studied. By the solvothermal process carried out at 140 °C, hexagonal, wurtzite phase $CuFeS_2$ was obtained with a phase fraction as high as ~92 wt%. A relatively, simple and low-temperature precipitation process using $(NH_4)_2S$ and distilled water produced micro- and nano-crystalline $CuFeS_2$ with various shapes including rods, hexagonal plates, and spheres etc. The synthesis methods reported here are believed to be beneficial for the further development of $CuFeS_2$ in the field of nanotechnology.

Keywords Diamond-like semiconductor · Polymorphs · Wurtzite · Chalcopyrite

1 Introduction

The developments of *nanoscience and nanotechnology* have allowed scientists to realize newer functionalities of (even previously known) materials and improve the efficiency of preparing the materials while reducing production cost [1]. Irrespective of the technology that is involved, large-scale, bulk production is a proven way to reduce the cost of the end-products. In the case of nanomaterials, the choice of synthetic route could be considered the first step toward low-cost end-products. Essentially, the synthesis/production of various kinds of nanomaterials/nanostructures and their characteristic studies is still an active area of research [2]. For semiconductor nanocrystals/nanostructures, the ability to tune the optical band gap in the quantum confinement regime is appealing for finding applications in solar cells and other optoelectronic devices etc. [3]. These days, studies on high-quality nanocrystals and nanostructures of a few nanometers in size are often reported [4]. For example, the optical band gap of ZnS nanocrystals has been tuned over a span of 0.5 eV by reducing the size of the crystallites to a few

Electronic supplementary material The online version of this article (https://doi.org/10.1007/s42452-020-03729-4) contains supplementary material, which is available to authorized users.

✉ Balamurugan Karuppannan, kombaibala@gmail.com; ✉ Jennifer A. Aitken, aitkenj@duq.edu | [1]Department of Chemistry and Biochemistry, Duquesne University, Pittsburgh, PA 15282, USA. [2]2D Materials Laboratory, Department of Physics, National Institute of Technology, Tiruchirappalli, Tamil Nadu 620015, India. [3]Department of Physics, Alagappa University, Karaikkudi, Tamil Nadu 630003, India. [4]RJ Lee Group Inc., Monroeville, PA 15146, USA.

nanometers [5]. Similarly, Yu et al. have shown how the dimensionality of the quantum confinement changes the band gap and exciton wavelength in InP nanocrystals [6]. Yet another interesting report from Yong et al. presents PbSe nanocrystals having various exotic shapes [7].

Chalcopyrite ($CuFeS_2$) is a naturally existing mineral that crystallizes in the noncentrosymmetric, tetragonal space group $I\bar{4}2d$, with lattice constants, $a = 5.289$ (1) Å and $c = 10.423$ (1) Å [8]. The crystal structure of the chalcopyrite $CuFeS_2$ is shown in Fig. 1a. The tetragonal, chalcopyrite structure can be derived from the cubic structure of zinc blende (ZnS). In $CuFeS_2$, the Cu^+ and Fe^{3+} metal cations have tetrahedral coordination with the S^{2-} anions. The CuS_4 and FeS_4 tetrahedra of $CuFeS_2$ are ordered in the 3D crystal lattice, such that the cubic symmetry ($F\bar{4}3m$) of the zinc blende structure is reduced to the tetragonal symmetry ($I\bar{4}2d$) by nearly doubling the unit cell along the *c*-axis. Moreover, the S^{2-} anions undergo a displacement, which contracts the *c*-axis of the unit cell, such that the *c*/*a* ratio is less than 2. Therefore, in a perfectly ordered structure of $CuFeS_2$, the Cu, Fe and S atoms occupy the 4a (0, 0, 0), 4b (0, 0, $\frac{1}{2}$) and 8d (0.2574, $\frac{1}{4}$, $\frac{1}{8}$) sites of the unit cell, respectively [8]. A typical *c*/*a* ratio of about 1.971 [8] is an indicative parameter of the tetragonality of the chalcopyrite structure.

The chalcopyrite $CuFeS_2$ is one of the many technologically important diamond-like semiconductor materials having the general formula I-III-VI_2, where I, III and VI represent the number of valence electrons of the atoms. Chalcopyrite type $CuFeS_2$ exhibits *n*-type semiconducting properties with a relatively narrow optical energy band gap (E_g) of 0.5–0.6 eV [9] and antiferromagnetic ordering below its Néel temperature, $T_N = 823$ K [10]. Even though the chalcopyrite $CuFeS_2$ has been known for quite a long time, a dispute about the ordering of magnetic moment of Cu has only been recently resolved [11]. Several relatively recent reports show that nanocrystalline $CuFeS_2$ can be used to improve the performance of the devices and often displays enhanced physicochemical properties compared to that of the bulk material. For example, Nengtao et al. [12] have demonstrated the detection of bioactive cations (Cu^{2+} and Fe^{3+}), with high selectivity and sensitivity, by $CuFeS_2$ quantum dots [12].

In the literature, dye sensitized solar cells (DSSC) with a counter electrode (CE) made of cubic (zincblende type) $CuFeS_2$ nanocrystals have been found to exhibit slightly higher (8.10%) power conversion efficiency than that of a DDSC having a Pt CE [13]. The use of thin film chalcopyrite $CuFeS_2$ nanocrystals as a hole transport layer in cadmium telluride (CdTe) solar cells brought its efficiency to ~12% [14]. The photo-thermal (light-to-heat) conversion property of colloidal chalcopyrite $CuFeS_2$ nanocrystals (with 49% efficiency), when exited by a near infrared laser ($\lambda = 808$ nm), within the biological window of $\lambda = 650$–900 nm (in which the light has more depth of penetration into tissues), has been reported by Sandeep

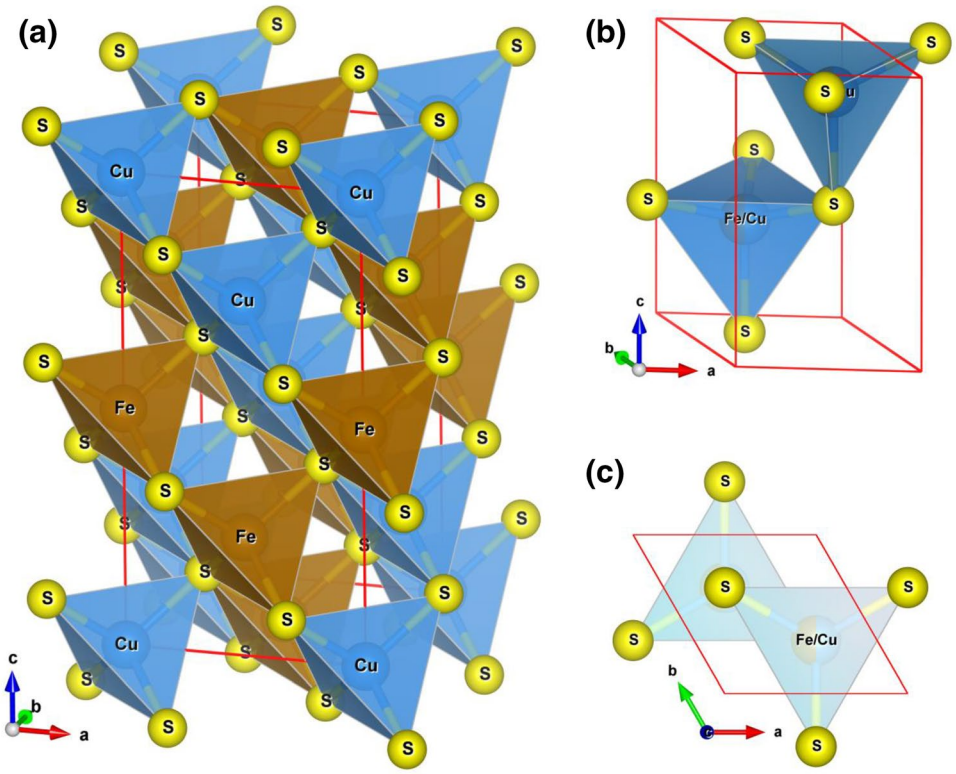

Fig. 1 Crystal structures of $CuFeS_2$: (**a**) tetragonal ($I\bar{4}2d$), chalcopyrite phase and (**b**, **c**) hexagonal ($P6_3mc$), wurtzite phase

et al. [15]. Chalcopyrite $CuFeS_2$ nanocrystals synthesized using a facile, solution-phase method have been found to exhibit enhanced thermoelectric performance ($ZT = 0.264$ at 500 K), 77 times the value of bulk chalcopyrite [16].

In this article, we present an interesting work involving in the synthesis of micro- and nano-crystalline $CuFeS_2$ by low-temperature solvothermal and precipitation methods using a set of simple chemical reagents and procedures. We obtained nanocrystalline $CuFeS_2$ in various exotic shapes including prisms, hexagonal rods and plates, etc. More notably, a symmetry lowered, hexagonal, wurtzite phase $CuFeS_2$ (see Fig. 1b, c) was also obtained. Since lowering (or altering) the fundamental crystal symmetry of a material by utilizing synthetic degree of freedom is still an area ripe for development, we believe our work presents a timely achievement.

2 Experimental details

In the solvothermal method, aqueous solutions of 1 mmol CuCl (99.9%), 1 mmol $FeCl_3$ (99.99%) and 2.02 mmol $(NH_4)_2S$ (20–24 wt% from Fisher Scientific) were used. The reactant solutions were taken in a Parr bomb, Teflon autoclave enclosed by a stainless-steel outer vessel. Anhydrous ethylenediamine (en) of variable quantities, 1 to 4 ml, was used as the solvent. The reactant mixture was tightly closed in the Parr bomb and heated using a laboratory oven for 24 h. The solvent quantity and the reaction temperature were varied; two sets of samples corresponding to the reaction temperatures of 170 °C and 140 °C were obtained. The products of the reactions were separated from the residual liquids by filtering and washed further using deionized water to remove the NH_4Cl byproduct (see Eq. 1). The cleaned products were dried in air and black powders were obtained as the final products. The powder materials were annealed at different temperatures, resulting in different crystalline quality and microstructure.

$$CuCl(aq.) + FeCl_3(aq) + 2\left(NH_4\right)_2S(l) \xrightarrow{\Delta} CuFeS_2(s) + 4NH_4Cl(l) \quad (1)$$

In the precipitation method, 2 mmol CuCl and 2 mmol of $FeCl_3$ salts were taken in a conical flask (25 ml volume). Using a magnetic stirrer, the salts were dissolved in 5 ml of deionized water. Once a transparent, bluish-green solution was obtained at room temperature, the temperature of the solution was raised to 80 °C. A 4.04 mmol $(NH_4)_2S$ solution (diluted by 1:4 ratio with deionized water) was added slowly (for about 30 min) to the hot solution containing Cu^+ and Fe^{3+} ions. The addition of the dilute $(NH_4)_2S$ solution readily produced a black precipitate. [View the video ($CuFeS_2$ by precipitation method.wmv) found in the supplemental material]. The precipitate was kept at 80 °C for 1 h while it was continuously stirred. Thereafter, it was allowed to cool down to room temperature and settle overnight. Later the precipitate was repeatedly washed several times using deionized water by vacuum filtration using a porous funnel. Alternately, a portion of the sample was washed repeatedly by centrifuging using deionized water. The products were dried at room temperature for 1 day. The final products were annealed at different temperatures.

The crystallinity and phase purity of the synthesized materials were examined using an X'Pert Pro MPD X-ray powder diffractometer (*PANalytical*) operating in Bragg Brentano geometry and employing Cu K_α radiation. Using X-ray powder diffraction data, Rietveld refinements were performed for a set of selected samples using the General Structure Analysis System (GSAS) [17, 18]. Micrographs displaying the micro- and nanostructures of the samples were collected at 2.0 kV using an ultra-high-resolution Hitachi S5500 cold Field Emission in lens Scanning Electron Microscope (FESEM) by Hitachi High-Technologies Corp.

3 Results

3.1 $CuFeS_2$ nanocrystalline materials prepared by a solvothermal process

Figure 2 shows the X-ray powder diffraction patterns of four samples synthesized by a solvothermal reaction carried out at 170 °C for 24 h. The samples, S1, S2, and S3, were synthesized using 2, 3 and 4 ml of ethylenediamine (en) as the solvent, respectively. The sample S4 was obtained after annealing the sample S3 at 150 °C for 3 h. (See Table 1 for an outline of sample labeling, S1–S4, prepared by the solvothermal process.) An indexed X-ray powder diffraction pattern of polycrystalline, bulk chalcopyrite $CuFeS_2$ with tetragonal (T) structure is shown for reference. The X-ray powder diffraction pattern of S1 contains many additional peaks of considerably high intensity that cannot be indexed using the tetragonal $CuFeS_2$ phase. Rather, the X-ray powder diffraction pattern looks similar to that of nanocrystalline Cu-In-S with a wurtzite-type structure reported by Michelle et al. [20] and wurtzite-$CuInS_2$ hexagonal plates reported by Xia et al. [19]. Therefore, a two-phase model was employed for Rietveld refinement using both hexagonal, wurtzite-type and tetragonal, chalcopyrite-type $CuFeS_2$ structures. The X-ray powder diffraction data of S1 were reasonably fit using the combined two-phase model. A summary of the results of Rietveld analysis can be found in the supplemental material. The refined lattice constants of the wurtzite-phase $CuFeS_2$ are $a = 3.6971(8)$ Å and $c = 6.1672(2)$ Å. The refined weight

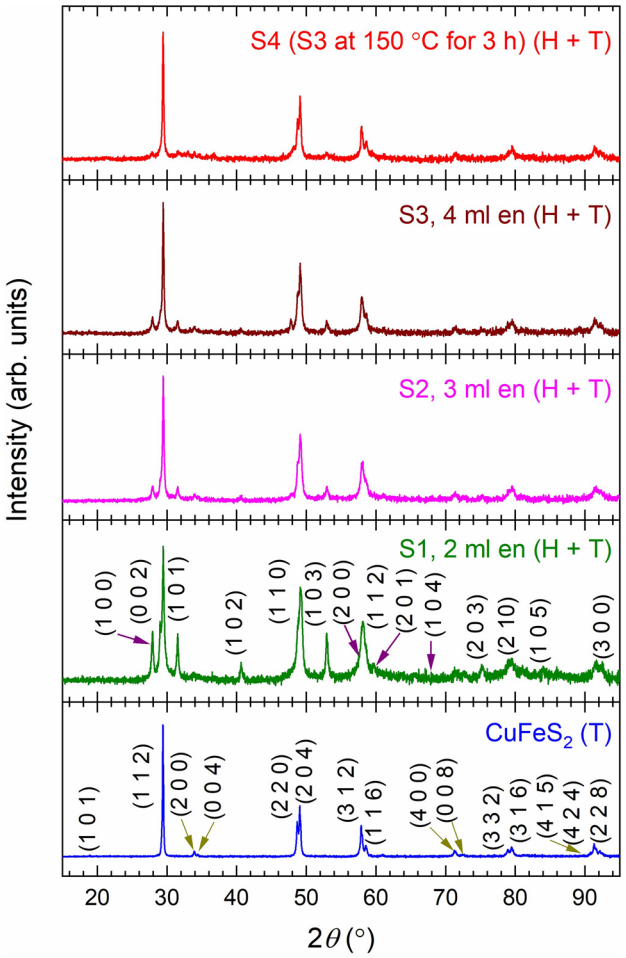

Fig. 2 The X-ray powder diffraction patterns of bulk polycrystalline $CuFeS_2$ with chalcopyrite, tetragonal (T) structure (bottom), nanocrystalline samples (S1, S2, S3, and S4) synthesized by solvothermal reaction at 170 °C for 24 h and different quantities of ethylenediamine (en). Here, (H+T) indicates that the sample contains both hexagonal, wurtzite-type and tetragonal, chalcopyrite phases. Sample S4 was obtained by annealing S3 at 150 °C for 3 h. The Miller indices given for bulk, tetragonal $CuFeS_2$ (T) [8], and that given for sample, S1 correspond to the hexagonal structure were obtained in the Rietveld analysis [19]

fractions of wurtzite and chalcopyrite phases for S1 are ~21 wt% and ~79 wt%, respectively. The unit cell of the hexagonal $CuFeS_2$ is shown in Fig. 1b, c. In this structure, both Cu and Fe atoms occupy the same crystallographic site (1/3, 2/3, 0.3934), each with an occupation factor of 0.5 and have tetrahedral coordination with the S atoms. The unit cell contains one formula unit.

From the X-ray powder diffraction analysis, we find that if the quantity of en is increased to 3 and 4 ml, the intensity of the diffraction peaks (see S2 and S3 in Fig. 2) corresponding to the hexagonal phase is reduced and that of the tetragonal phase is increased. Further, annealing the sample S3 at 150 °C for 3 h resulted in the growth of the tetragonal phase at the expense of the hexagonal phase (see S4 in Fig. 2).

Figure 3 shows the secondary electron (SE) images of the samples S1, S2, S3 and S4. It is evident that the concentration of the solvent, en, may be used to obtain nanocrystalline $CuFeS_2$ of different sizes and shapes, such as (hexagonal) rods (about 50 nm in diameter and longer in length), hexagonal plates (about 100 nm in width) (see Fig. 3a), various kinds of polygons (about 40 nm to 150 nm in size) (see Fig. 3b) and also some irregular shapes (with a crystallite of size about 100 nm to 170 nm or less) (see Fig. 3b, c). As one would normally expect, even though it is obtained by a low temperature and short time annealing (at 150 °C for 3 h), the sample S4 has ~7 times larger crystallites than S3 (see Fig. 3d).

The morphologies of the micro-/nanocrystalline $CuFeS_2$ are not limited to those shown in Fig. 3. Other representative SE images of the samples (S1, S2, S3 and S4) are shown in Fig. 4. In the solvothermal process, $CuFeS_2$ hexagonal rods of more than 1 μm in length and ~100 nm in diameter (see Fig. 4a,c) were obtained. Moreover, there were many twinned and untwinned polygons (see Fig. 4b, d, e) including hexagonal plates (see Fig. 4f, h) and many rod-like structures (see Fig. 4a, b, g). A $CuFeS_2$ prism, indicated by a schematic picture inserted in Fig. 4g, is another interesting nanostructure obtained by the solvothermal method. Similarly, the SE images of samples S5–S8 (for details, see Table 1), shown in Fig. 5, confirm the presence of $CuFeS_2$ micro- and nano-crystalline particles with many different shapes, such as rods, polygons, plates etc. Figure 5 also evidences that the sample S7 has a relatively higher fraction of hexagonal rod-like structures (see Fig. 5e, f). The sample S8 has no distinct microstructure; it appears as an aggregation of the particles (Fig. 5g, h).

The X-ray powder diffraction patterns of the samples S5, S6, S7 and S8 are shown in Fig. 6 with reference to that of the bulk, tetragonal (T), chalcopyrite $CuFeS_2$. It is evident that both the tetragonal, chalcopyrite and hexagonal, wurtzite phases of $CuFeS_2$ are present in all the samples. However, it is easily identified that sample S7 contains a relatively higher fraction of the hexagonal wurtzite phase. This is confirmed by the phase fractions of the hexagonal (~92 wt%) and tetragonal (~8 wt%) phases of $CuFeS_2$ obtained from the Rietveld analysis using the X-ray powder diffraction data of sample S7 (see Table S2 in supplement material).

3.2 $CuFeS_2$ nanocrystalline materials by precipitation process

Aqueous $(NH_4)_2S$ is a highly reactive reagent; it can readily produce sulfide derivatives of transition metals when added to an aqueous solution containing transition

Table 1 Synthetic details for $CuFeS_2$ nanocrystalline samples prepared by solvothermal process

Sample code	Solvent amount (en)	Reaction temperature	Reaction time	Post processing
S1	2 ml	170 °C	24 h	VFF
S2	3 ml	170 °C	24 h	VFF
S3	4 ml	170 °C	24 h	VFF
S4 (S3 annealed)	N.A.	N.A.	N.A.	CD + A
S5	1 ml	140 °C	24 h	CD
S6	2 ml	140 °C	24 h	CD
S7	3 ml	140 °C	24 h	CD
S8	4 ml	140 °C	24 h	CD

en ethylenediamine

VFF vacuum funnel filtered

CD centrifuged and dried in fume-hood for 2 days

A annealed at 150 °C for 3 h

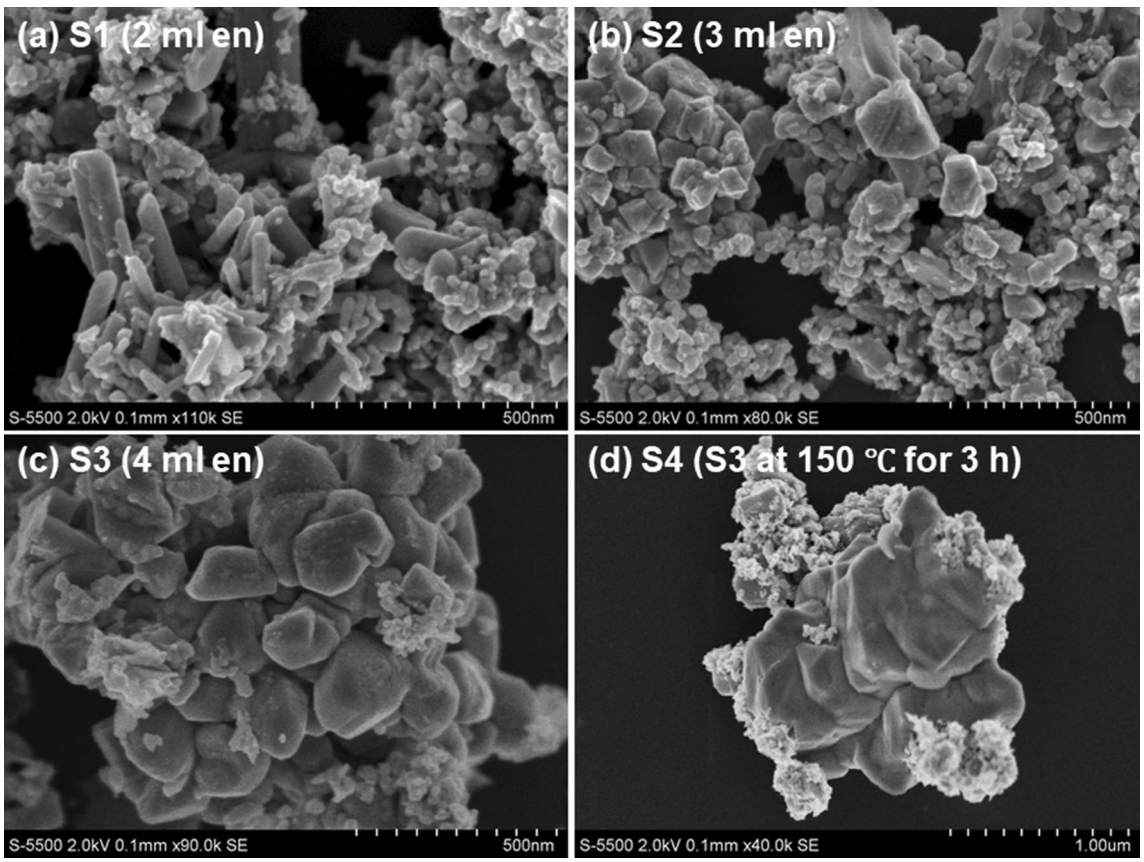

Fig. 3 Secondary electron images of the samples (**a**) S1, (**b**) S2, (**c**) S3 and (**d**) S4, showing the effect of solvent amount, ethylenediamine (en), and annealing (at 150 °C for 3 h) on the particle size and shape. (Other shapes of the nanoparticles are shown in Fig. 4). Note that the scale bars are not the same in all micrographs

metal cations. These transition metal sulfide molecules agglomerate and produce precipitates. If a small amount of heat energy is supplied to the precipitates produced in the reaction, nucleation and crystal growth occurs that eventually produce transition metal sulfide nanocrystals [21]. Interestingly, we could obtain nanocrystals of the ternary transition metal-sulfide, $CuFeS_2$ at relatively low-temperature, 80 °C, via this precipitation process. (Find a video-graphic summary, *$CuFeS_2$ by precipitation method.wmv*, given in the supplemental material.)

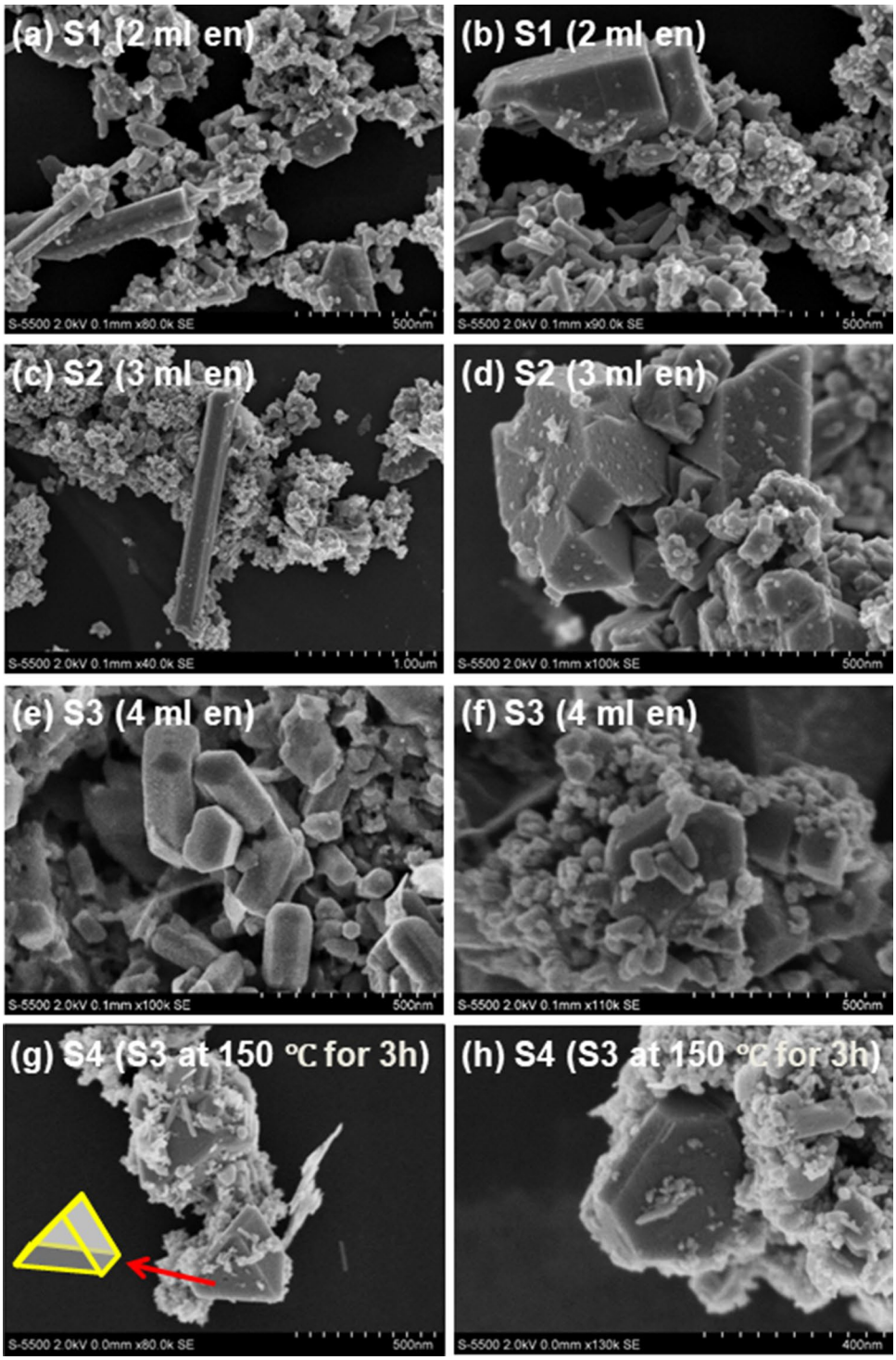

Fig. 4 Secondary electron images of the samples (**a**, **b**) S1, (**c**, **d**) S2, (**e**, **f**) S3 and (**g**, **h**) S4, showing various morphologies. (Note that the scale bars are not the same in all micrographs)

Figure 7 shows the X-ray powder diffraction patterns of the as-prepared $CuFeS_2$ obtained by the precipitation process (P1) and that of samples annealed (P2, P3 and P4) at various temperatures. (See Table 2 for an outline of sample labeling.) The X-ray powder diffraction pattern of sample P1 shows broad peaks matching the expected Bragg reflections for bulk chalcopyrite $CuFeS_2$. There are a few barely distinguishable diffraction-peaks corresponding to the wurtzite-type $CuFeS_2$. Moreover, there are some additional peaks, which cannot be indexed to either the chalcopyrite or wurtzite $CuFeS_2$. These unknown peaks are suppressed almost completely by annealing at 150 °C for 24 h, but some new unidentified peaks are produced. The relatively sharper peaks in the

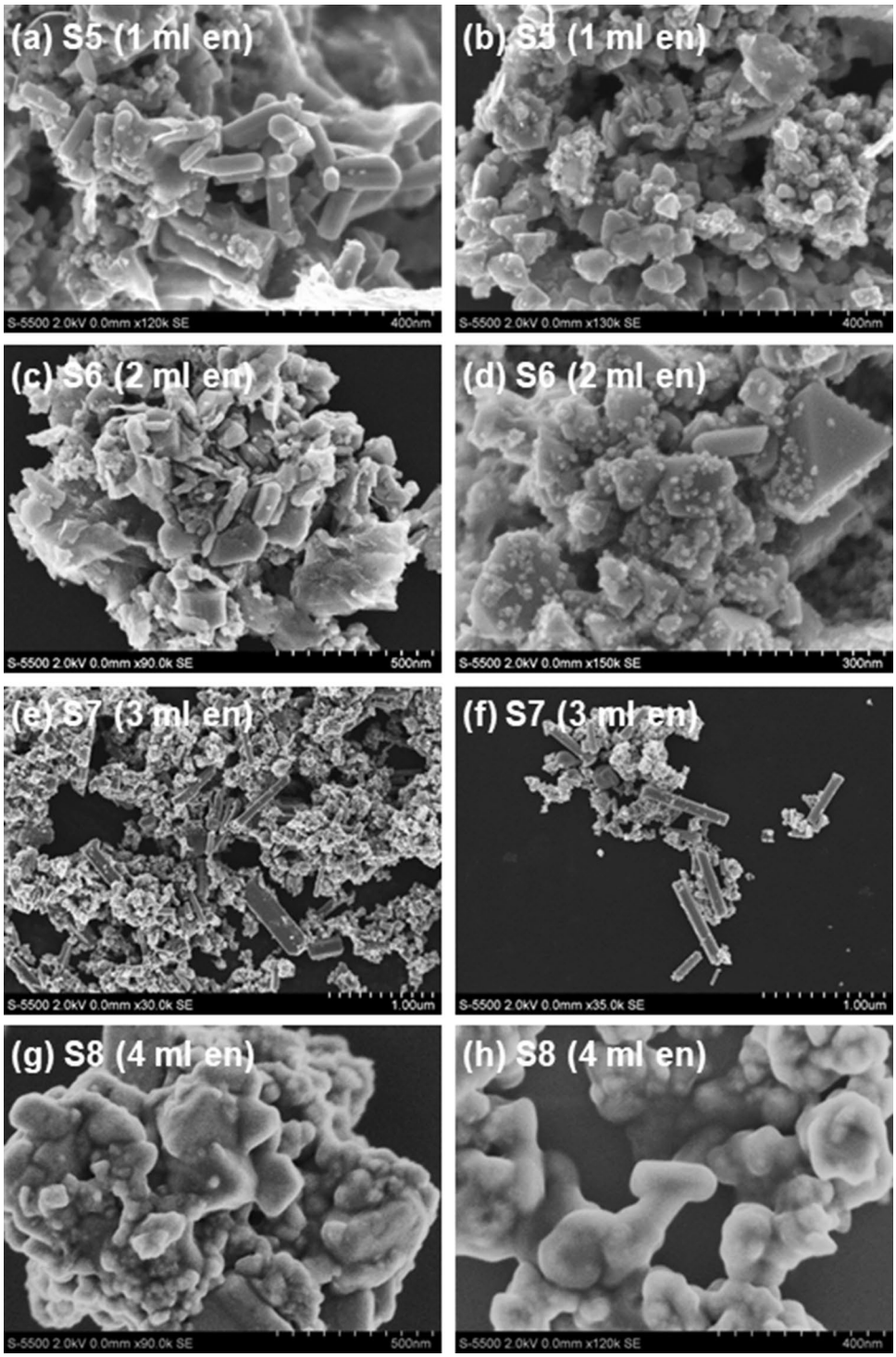

Fig. 5 Secondary electron images of the samples (S5, S6, S7 and S8) synthesized by a solvothermal reaction carried out at 140 °C for 12 h using 1, 2, 3 and 4 ml of solvent, ethylenediamine (en) respectively. (Note that the scale bars are not the same in all micrographs)

X-ray powder diffraction data of the sample P2, is likely due to the greater presence of micron-sized particles. It should be noted that the sample P2 was obtained by centrifuging and annealing at 150 °C for 3 h, while the two other samples P3 and P4 were obtained by vacuum filtration and annealing at 150 °C for 12 h and 24 h respectively.

Figure 8 shows the SE images of the samples P1, P2, P3 and P4. The as-prepared sample (P1) contains agglomerated nanoparticles lacking a regular shape (see Fig. 8a); yet there are some spherical particles with sizes as small as 30 nm (see Fig. 8b). Annealing has an interesting effect on the morphology of the particles (see Fig. 8c–h). The sample, P2, annealed at 150 °C for

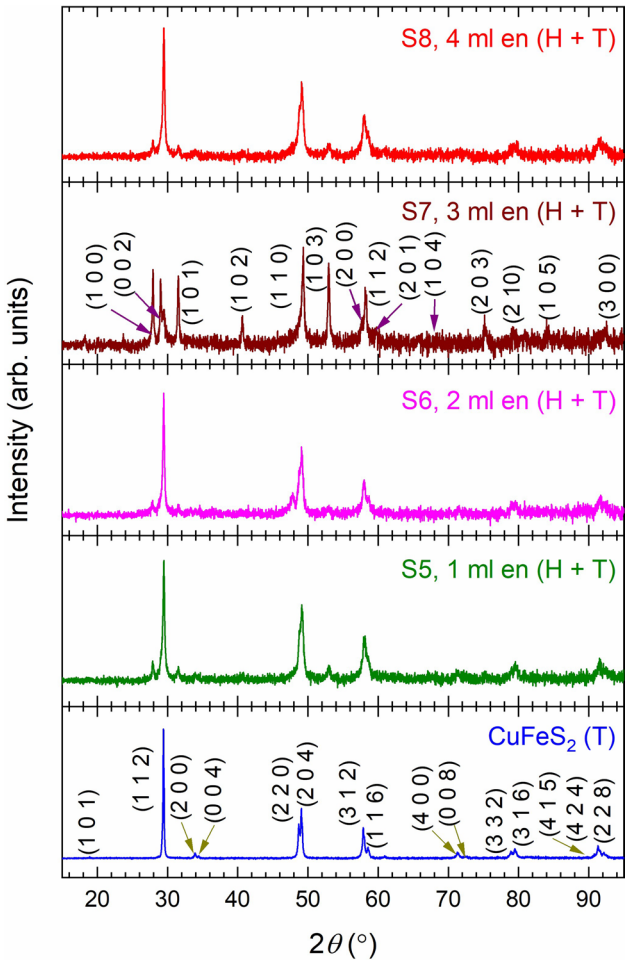

Fig. 6 The X-ray powder diffraction patterns of bulk polycrystalline $CuFeS_2$ with chalcopyrite, tetragonal (T) structure (bottom), nanocrystalline samples (S5, S6, S7, and S8) synthesized by solvothermal reaction at 140 °C for 24 h and different quantities of ethylenediamine (en). Here, (H + T) indicates that the sample contains both hexagonal, wurtzite-type and tetragonal, chalcopyrite phases. The Miller indices given for bulk, tetragonal $CuFeS_2$ (T) [8], and that given for sample, S7 corresponding to the hexagonal structure were obtained in the Rietveld analysis [19]

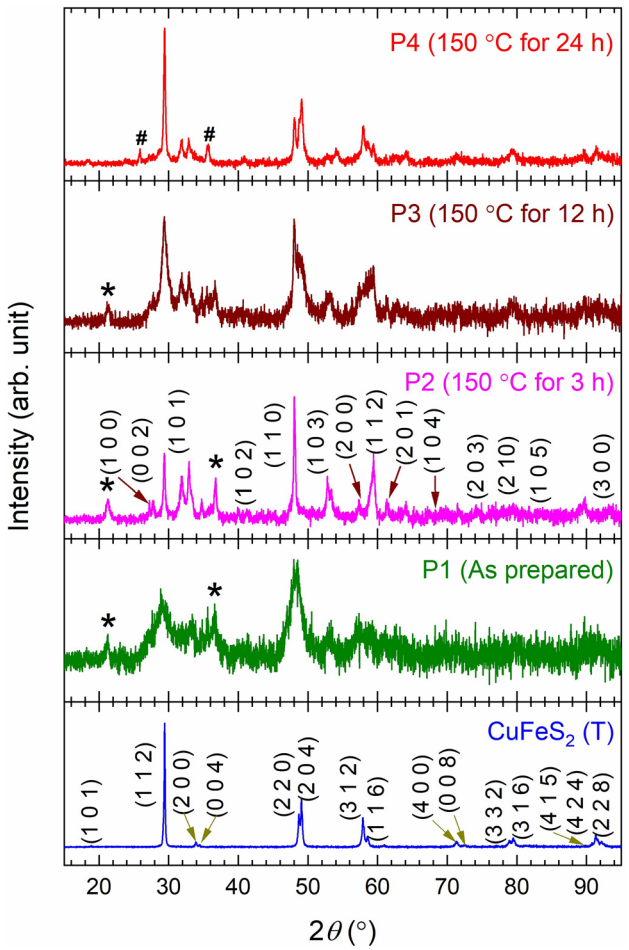

Fig. 7 X-ray powder diffraction patterns of bulk polycrystalline $CuFeS_2$ with chalcopyrite, tetragonal (T) structure (bottom) and nanocrystalline $CuFeS_2$ sampels synthesized by precipitation process carried out at 80 °C for 1.5 h. Except P1, other samples (P2, P3, and P4) were annealed at 150 °C for 3, 12 and 24 h respectively. The Miller indices given for bulk, tetragonal $CuFeS_2$ (T) [8], and that given for sample, P2 corresponding to the hexagonal structure were obtained in the Rietveld analysis [19]. The peaks indicated by * and # belong to unidentified phase(s)

3 h, contains mostly rod-like particles of ~200 nm in length or longer (see Fig. 8c). The same sample also contains a few hexagonal plates (see Fig. 8d). This is likely the wurtzite-type $CuFeS_2$, which is evident in the X-ray powder diffraction patterns, as discussed above. The sample P3, annealed at 150 °C for 12 h, contains agglomerated rod-like particles, as well as hexagonal plates and some irregularly shaped particles (see Fig. 8e, f). As shown in Fig. 8g, h, annealing at 150 °C for 24 h seems to hinder the formation of any regularly shape particles and the crystallites grow in size.

Table 2 Synthetic details for $CuFeS_2$ nanocrystalline samples prepared by precipitation process

Sample code	[a]Reaction condition	Post processing
P1	At 80 °C for 1.5 h[a]	VFF
P2 (P1 annealed)	N.A.	CD + A (3 h)
P3 (P1 annealed)	N.A.	VFF + A (12 h)
P4 (P1 annealed)	N.A.	VFF + A (24 h)

[a]Time, taken to add the diluted $(NH_4)_2S$ into the solution containing Cu^+ and Fe^{3+} cations

VFF vacuum funnel filtered.

CD centrifuged and dried in fume-hood for 2 days

A annealed at 150 °C

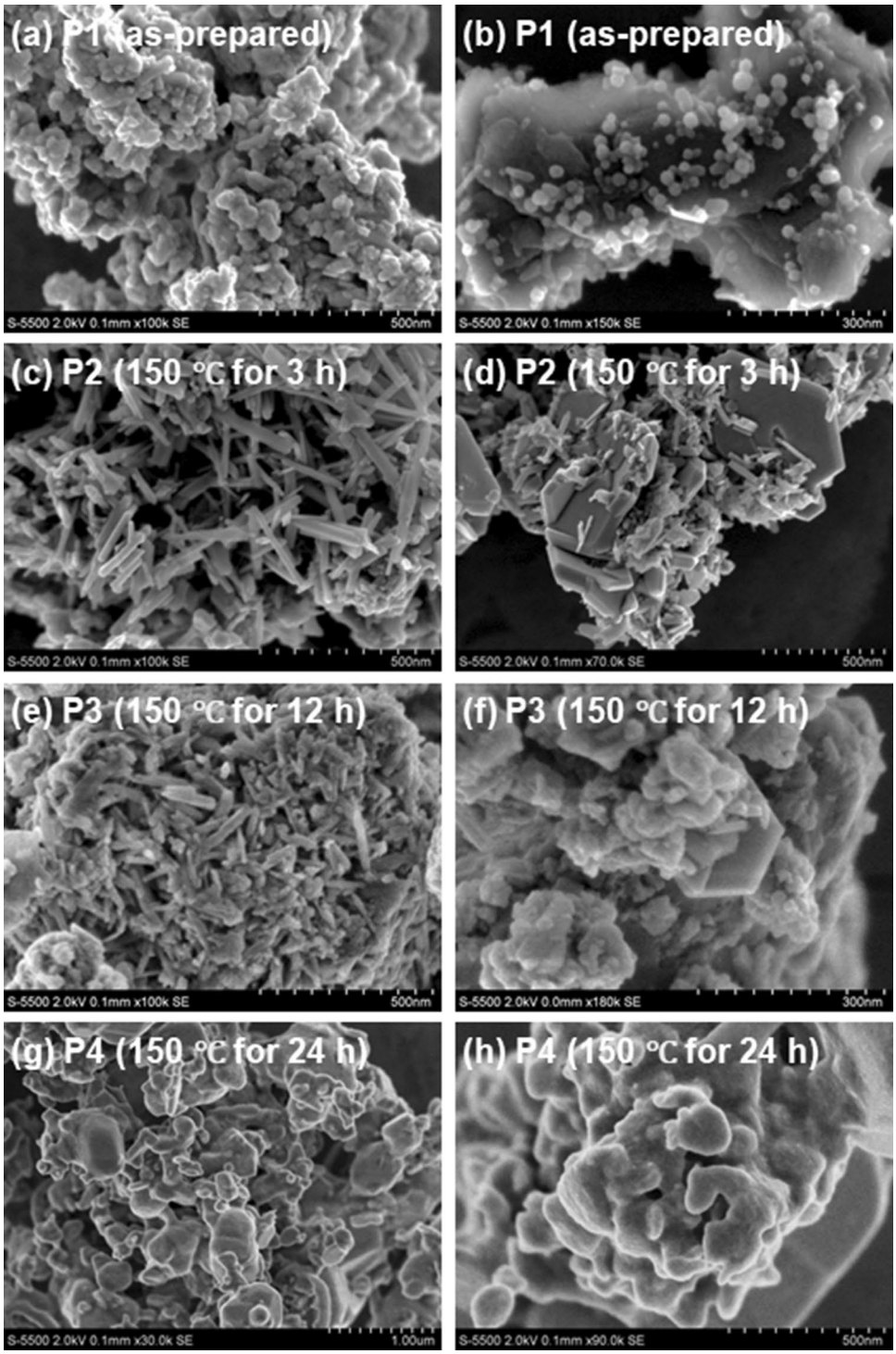

Fig. 8 Secondary electron images of the nanocrystalline $CuFeS_2$ samples synthesized by precipitation process carried out at 80 °C for 1.5 h. (**a**, **b**) P1 is the as-prepared sample (without annealing). (**c**, **d**) P2, (**e**, **f**) P3 and (**g**, **h**) P4 are the samples annealed at 150 °C for 3 h, 12 h and 24 h respectively. (Note that the scale bars are not the same in all micrographs)

4 Discussion

In the past research works, nanocrystalline $CuFeS_2$ materials were mostly synthesized by a solvothermal [22, 23] or a hydrothermal [24] process employing different reagents. To the best of our knowledge, there are no reports in the literature that present low temperature synthesis of micro- and nano-crystalline $CuFeS_2$ materials using very simple reagents like those reported here. Additionally, our procedures have resulted in $CuFeS_2$ with various exotic morphologies. The results of Prashant et al. [25] and Yaser et al. [26] compare to some extent, with those reported here; in that, the mixed phases of chalcopyrite (tetragonal) and wurtzite (hexagonal) $CuFeS_2$ polymorphs were found.

However, Prashant et al. have only reported flower-like morphology, while, Yaser et al have only reported polyhedral-shaped nanocrystals.

From our work, we understand that both the volume of the solvent (en) and the reaction temperature of the solvothermal process are crucial to stabilize the wurtzite-type $CuFeS_2$. Basically, lowering the reaction temperature requires relatively higher volume of en to grow wurtzite-type $CuFeS_2$. On the other hand, the precipitation process produced tetragonal chalcopyrite phase with the least amount of wurtzite-type $CuFeS_2$. The unknown and unwanted phase obtained in the precipitation process can be eliminated if the reaction is carried out at slightly higher temperature followed by annealing.

We outline a probable reaction sequence for the formation of the wurtzite-phase $CuFeS_2$ as follows. In the first step, metastable mono-sulfides, CuS (called *covellite*) [27] and FeS (called *troilite*) [28, 29], both with hexagonal symmetry, are formed just like the mono-sulfide of zinc, ZnS with hexagonal (wurtzite) structure. In the second step, powered by the heat energy supplied for the reaction, the transition metal cations of Cu and Fe in the metastable mono-sulfides diffuse across their interface and form the $CuFeS_2$ product. Ultimately, the final product $CuFeS_2$ ends up having hexagonal symmetry of the wurtzite structure.

The low-temperature synthesis procedures described here were also tested to synthesize nanocrystalline $CuInS_2$. The corresponding results were presented elsewhere [30]. Similarly, the wurtzite and chalcopyrite phases of $CuInS_2$ could be obtained via a synthetic procedure using a simple solution route like that reported by Xia et al. [19]. Further, a review by Dmitry et al. [4] points out that many ternary and quaternary metal chalcogenide nanocrystals can be synthesized in various exotic shapes. The review article describes the formation of spherical as well as pyramidal chalcopyrite $CuFeS_2$ [31]; however, the synthetic procedures outlined there are not as simple as those that we have reported. Therefore, we believe that the work reported here outlines a promising, low-temperature synthesis route to obtain technologically important metal chalcogenide nanocrystals.

5 Conclusion

We have developed two low-temperature procedures for synthesizing a technologically important class of ternary diamond-like semiconductor materials of the formula I-III-VI_2. The low-energy, solvothermal reaction process (170 °C and 140 °C), allowed access to a hexagonal, wurtzite-type $CuFeS_2$ micro- and nano-crystals together with the tetragonal, chalcopyrite $CuFeS_2$ nanocrystals. It has been found that the volume of the solvent, (en) and the reaction temperature, both have important role in the relative amount of wurtzite-type $CuFeS_2$ nanocrystals produced in the synthesis. On the other hand, a low-temperature (80 °C) precipitation process was found to produce mostly the chalcopyrite phase, with the least amount of wurtzite phase $CuFeS_2$ nanocrystals. The interesting results and great potential of the synthesis procedures discussed here are to be explored further towards obtaining monodisperse, phase-pure nanocrystals of specific shapes and sizes. We have already demonstrated that the method can be used for $CuInS_2$. We believe that these low-temperature synthesis procedures could be easily extended to other ternary and quaternary diamond-like semiconductor nanocrystals such as $CuInTe_2$ and $CuInSe_2$, etc.

Acknowledgements Dr. K. Balamurugan acknowledges the Department of Science and Technology (DST), Ministry of Science and Technology, Government of India for Innovation in Science Pursuit for Inspired Research (INSPIRE) Faculty Award and Research Grant (IFA14-PH-91), and also NIT Tiruchirappalli for hosting as an INSPIRE Faculty and providing space to set up "2D Materials Laboratory". Dr. K. Balamurugan and Prof. Dr. G. Ravi acknowledge Ministry of Human Resource Development (MHRD), Government of India for funding under RUSA 2.0 (Rashtriya Uchchattar Shiksha Abhiyan - National Mission for Higher Education). Dr. J. Aitken acknowledges support from the United States National Science Foundation, Division of Materials Research, Under Grant number DMR 1201729. Dr. J. Aitken acknowledges support from the Bayer School of Natural and Environmental Sciences at Duquesne University for allowing her to conduct a sabbatical at R J Lee Group.

Compliance with ethical standards

Conflict of interest The authors have no conflicts of interest.

References

1. Anne P, Bernier P, Lannoo M (2011) Recent developments in nanoscience and nanotechnology. Adv Mater Res 324:3–7
2. Brian LC, Vladimir LK, Charles JO (2004) Recent advances in the liquid-phase syntheses of inorganic nanoparticles. Chem Rev 104:3893–3946
3. Andrew MS, Shuming N (2010) Semiconductor nanocrystals: structure, properties, and band gap engineering. Acc Chem Res 43:190–200
4. Dmitry A, Aurélie L, Peter R (2013) Ternary and quaternary metal chalcogenide nanocrystals: synthesis, properties and applications. J Mater Chem C 1:3756–3776
5. Nanda J, Sameer S, Sarma DD, Nirmala C, Gary H (2000) Size-selected zinc sulfide nanocrystallites: synthesis, structure, and optical studies. Chem Mater 12:1018–1024
6. Heng Y, Jingbo L, Richard AL, Lin-Wang W, William EB (2003) Two- versus three-dimensional quantum confinement in indium phosphide wires and dots. Nat Mater 2:517–520
7. Ken-Tye Y, Yudhisthira S, Kaushik RC, Mark TS, John RM, Paras NP (2006) Shape control of PbSe nanocrystals using noble metal seed particles. Nano Lett 6:709–714
8. Hall SR, Stewart JM (1973) The crystal structure refinement of chalcopyrite, $CuFeS_2$. Acta Cryst B 29:579–585

9. Wang MX, Wang LS, Yue GH, Wang X, Yan PX, Peng DL (2009) Single crystal of $CuFeS_2$ nanowires synthesized through solventothermal process. Mater Chem Phys 115:147–150
10. Woolley JC, Lamarche A-M, Lamarche G, Quintero M, Swainson IP, Holden TM (1996) Low temperature magnetic behaviour of $CuFeS_2$ from neutron diffraction. J Magn Magn Mater 162:347–354
11. Lovesey SW, Knight KS, Detlefs C, Huang SW, Scagnoli V, Staub U (2012) Acentric magnetic and optical properties of chalcopyrite ($CuFeS_2$). J Phys Condens Matter 24:216001
12. Nengtao W, Xingyu L, Min Z, Jinwei G, Xubing L, Zhi Z, Yuhui Z (2019) Controllable synthesis of novel luminescent $CuFeS_2$ quantum dots with magnetic properties and cation sensing features. J Nanopart Res 21:268
13. Yihui W, Bin Z, Chi Y, Shichao L, Wen-Hua Z, Can L (2016) $CuFeS_2$ colloidal nanocrystals as an efficient electrocatalyst for dye sensitized solar cells. Chem Commun 52:11488–11491
14. Ebin B, Khagendra PB, Indra S, Nikolas JP, Randy JE (2018) Structural, optical, and hole transport properties of earth-abundant chalcopyrite ($CuFeS_2$) nanocrystals. MRS Commun 8:970–978
15. Sandeep G, Tommaso A, Alessia P, Ilka K, Gaspari R, Almeida G, Giovanni B, Andrea C, Francesco S, Teresa P, Liberato M (2016) Colloidal $CuFeS_2$ nanocrystals: intermediate Fe d-band leads to high photothermal conversion efficiency. Chem Mater 28:4848–4858
16. Daxin L, Ruoshui M, Shihui J, Guangsheng P, Shouhua F (2012) A facile synthetic approach for copper iron sulfide nanocrystals with enhanced thermoelectric performance. Nanoscale 4:6265–6268
17. Larson AC, von Dreele RB (1994) General structure analysis system (GSAS). Los Alamos National Laboratory Report LAUR 86–748
18. Toby BH (2001) EXPGUI, a graphical user interface for GSAS. J Appl Crystallogr 34:210–213
19. Xia S, Lei W, Yeping L, Deren Y (2011) Synthesis of hexagonal structured wurtzite and chalcopyrite $CuInS_2$ via a simple solution route. Nanoscale Res Lett 6:562
20. Michelle EN, Matthew AF, Richard LB (2009) Growth kinetics of monodisperse Cu-In-S nanocrystals using a dialkyl disulfide sulfur source. Chem Mater 21:4299–4304
21. Clemens B, Xiaobo C, Radha N, Mostafa AE (2005) Chemistry and properties of nanocrystals of different shapes. Chem Rev 105:1025–1102
22. Junqing H, Qingyi L, Kaibin T, Yitai Q, Guien Z, Xianming L (1999) A solvothermal reaction route for the synthesis of $CuFeS_2$ ultrafine powder. J Mater Res 14:3870–3872
23. Yang J, Yue W, Xiao M, Weichao Y, Yi X, Yitai Q (2000) Elemental solvothermal reaction to produce ternary semiconductor $CuInE_2$ (E = S, Se) nanorods. Inorg Chem 39:2964–2965
24. Junqing H, Qingyi L, Bin D, Kaibin T, Yitai Q, Yuzhi L, Guien Z, Xianming L (1999) A hydrothermal reaction to synthesize $CuFeS_2$ nanorods. Inorg Chem Commun 2:569–571
25. Prashant K, Sitharaman U, Rajamani N (2013) Precursor driven one pot synthesis of wurtzite and chalcopyrite $CuFeS_2$. Chem Commun 49:7316–7318
26. Yaser V, Seyed MM, Muhammad NT, Reza G, Wolfgang T (2017) Synthesis of $CuFeS_2$ nanoparticles by one-pot facile method. J Nanostruct 7:284–291
27. Evans HT, Judith AK (1976) Crystal structure refinement of covellite. Am Mineral 61:996–1000
28. Alistair RL, David JV (1996) Spectroscopic studies of iron sulfide formation and phase relations at low temperatures, mineral spectroscopy; a tribute to roger G. Burns. The Geochemical Society, Special Publication No 5
29. Craco L, Faria JLB, Leoni S (2017) Electronic reconstruction of hexagonal FeS: a view from density functional dynamical mean-field theory. Mater Res Express 4:036303
30. Balamurugan K, Jacqueline S, Johanna B, Kristin B, Karen H, Jennifer A (2011) Micro- and nano-structures of I-III-VI_2-based materials prepared via solvothermal processes, Materials Science & Technology 2011 Conference & Exhibition (MS&T'11), Columbus, Ohio (USA) –Abstract link: http://www.programmaster.org/PM/PM.nsf/ApprovedAbstracts/70D4CE66024EE444852578540063424D?OpenDocument
31. Yu-Hsiang AW, Ningzhong B, Arunava G (2010) Shape-controlled synthesis of semiconducting $CuFeS_2$ nanocrystals. Solid State Sci 12:387–390